Biophysical Journal
Article

Biophysical Society

sw ApoMb Amyloid Aggregation under Nondenaturing Conditions: The Role of Native Structure Stability

Natalya S. Katina,[1] Vitalii A. Balobanov,[1] Nelly B. Ilyina,[1] Victor D. Vasiliev,[1] Victor V. Marchenkov,[1] Anatoly S. Glukhov,[1] Alexey D. Nikulin,[1] and Valentina E. Bychkova[1,*]
[1]Institute of Protein Research, Russian Academy of Sciences, Pushchino, Moscow Region, Russia

ABSTRACT Investigation of the molecular mechanisms underlying amyloid-related human diseases attracts close attention. These diseases, the number of which currently is above 40, are characterized by formation of peptide or protein aggregates containing a cross-β structure. Most of the amyloidogenesis mechanisms described so far are based on experimental studies of aggregation of short peptides, intrinsically disordered proteins, or proteins under denaturing conditions, and studies of amyloid aggregate formations by structured globular proteins under conditions close to physiological ones are still in the initial stage. We investigated the effect of amino acid substitutions on propensity of the completely helical protein sperm whale apomyoglobin (sw ApoMb) for amyloid formation from its structured state in the absence of denaturing agents. Stability and aggregation of mutated sw ApoMb were studied using circular dichroism, Fourier transform infrared spectroscopy, x-ray diffraction, native electrophoresis, and electron microscopy techniques. Here, we demonstrate that stability of the protein native state determines both protein aggregation propensity and structural peculiarities of formed aggregates. Specifically, structurally stable mutants show low aggregation propensity and moderately destabilized sw ApoMb variants form amyloids, whereas their strongly destabilized mutants form both amyloids and nonamyloid aggregates.

INTRODUCTION

In the last two decades, a considerable progress has been achieved in studies of amyloid aggregation (1–5). Currently, more than 40 diseases are known to be amyloid-related, including Alzheimer's disease, Parkinson's disease, type 2 diabetes, and others (1,2,6). These are associated with deposition in organs and tissues of amyloids, which are highly structured protein fibrils containing the cross-β structure (7). Amyloidogenesis is a multistep process that is problematic for experimental study, and therefore the molecular mechanism of protein aggregation is still poorly understood, and amyloid-related diseases remain almost incurable.

Amyloid aggregation has long been the subject of medical research. Some years ago, it was found that there are proteins apart from those immediately involved in disease-causing amyloidogenesis, including α-helical proteins, which are capable of generating amyloids under conditions specific to each case (8–10). Aggregates formed by these proteins can be as toxic to the cell as those of disease-related proteins, which points to certain common structural features of the aggregates as the toxicity source. Accordingly, it was concluded that amyloid formation is a common characteristic of polypeptide chains (8,9). Therefore it is possible to study features of the amyloid formation process using different proteins uninvolved in any disease. Thus investigations of protein aggregates and their kinetic and thermodynamic characteristics became a research subject of molecular biophysics. Three types of acylphosphatase, HypF-N, horse and sperm whale apomyoglobins, B1 immunoglobulin-binding domain of protein G, and others were used as model proteins (3,11–16).

It was shown that nonnative protein conformations were aggregate precursors and therefore destabilization of protein structure was prerequisite and determinant for aggregation propensity to amyloid deposition (1,16–21). Therefore, in most subsequent studies, denaturing conditions such as high temperature or low pH, and addition of different denaturants and organic solvents were used that provided destabilization of protein structure and unfolding of the polypeptide chain (14,22–24). It was shown that for unfolded polypeptide chains, the physicochemical properties of amino acid residues produce the major effect on

Submitted December 6, 2016, and accepted for publication July 20, 2017.
*Correspondence: bychkova@vega.protres.ru
Editor: Daniel Raleigh.
http://dx.doi.org/10.1016/j.bpj.2017.07.011

protein amyloidogenicity, which increases with enhanced hydrophobicity and β-sheet propensity, and decreases the total charge of amyloidogenic regions in mutants (25–29). These results underlie most of the available algorithms for prediction of the effect of amino acid substitutions on the amyloidogenicity of proteins (30–33).

To gain a better understanding of in vivo protein aggregation and develop an approach to its regulation in the cell, it is necessary to reveal the features of aggregation under conditions close to physiological ones. Currently, such studies are not common, and the data offered in the literature are insufficient to characterize aggregate formation by structured proteins (12,13,34–38). Therefore, our goal was to reveal what factors affect amyloidogenicity of a globular protein under nondenaturing conditions. We selected sperm whale apomyoglobin (sw ApoMb) as a model in our research because the process of its folding and the structures of its conformational states have been studied in detail (39–45). In addition, it is a completely α-helical protein, which makes its conformational rearrangements accompanied by β-structure emergence most fascinating. Myoglobin is a single-domain, globular protein containing eight helices lettered from A to H (44). Its folding proceeds through an intermediate known as "the molten globule state," where A-, G-, H-, and partially B-helices are structured, whereas the other helices fluctuate (42–44).

To date, the mechanism of ApoMb amyloid aggregation remains unclear. It has been shown that unfolded horse ApoMb is capable of forming fibrils under denaturing conditions (60°C and pH 9) (14); further, the double substitution of sw ApoMb W7FW14F inducing pronounced protein destabilization causes generation of amyloids even at room temperature (15,46,47). Our goal was to investigate sw ApoMb aggregation under conditions maximally close to physiological ones. Previously, we reported that 40°C and pH 5.5 were the conditions under which this protein, in its structured state, was capable of forming fibrils (37). Here, we investigated the effect of amino acid substitutions on sw ApoMb amyloid aggregation under these conditions. Eleven mutants of this protein were constructed, and their stability and properties of the formed aggregates were investigated using a wide range of biophysical techniques.

Currently, a broad variety of aggregate conformations produced by polypeptide chains, where amyloids are only one type of known protein aggregates, are available in the literature (48). To understand the mechanisms of not only amyloidogenesis, but also the whole process of aggregate formation of sw ApoMb, we have studied the propensity of its mutant forms to form aggregates regardless of their structure and, separately, its amyloid-forming propensity. This approach allowed for finding two different pathways of sw ApoMb aggregation under the same solvent conditions. Both the aggregation propensity and structural characteristics of the aggregates were shown to be determined by the stability of the protein's native state. Specifically, structurally stable mutants show low aggregation propensity and moderate destabilization of the protein structure results in amyloid formation, whereas strongly destabilized mutants produce both amyloid and nonamyloid aggregates. In addition, this study has revealed that in contrast to aggregation of unfolded polypeptide chains, amyloidogenicity of sw ApoMb under nondenaturing conditions is not influenced by hydrophobicity and β sheet propensity of the substituting amino acid residues. Our data provided new, to our knowledge, information on the aggregation process of sw ApoMb from its structured state and the factors determining the aggregation pathway of this protein.

MATERIALS AND METHODS

Protein expression and isolation

Plasmids containing genes of sw ApoMb mutated forms were obtained using a 7QuikChange site-directed mutagenesis kit (Stratagene), with the plasmid pET_{17b} as a template (a kind gift from P.E. Wright) (49). sw ApoMb and its variants were isolated and purified as described previously, after expression of appropriate plasmids in *Escherichia coli* BL21 (DE3) cells (50).

Aggregation conditions

For the formation of amyloid structures, lyophilized proteins were dissolved in 10 mM of sodium phosphate buffer (pH 5.5), and centrifuged using a Beckman 100 ultracentrifuge (Beckman Coulter, Brea, CA) at 70,000 Rpm for 30 min at 4°C, to remove poorly dissolved material. Protein concentrations were determined spectrophotometrically. The extinction coefficient was calculated from the amino acid sequence and taken to be 0.88 for wild-type sperm whale apomyoglobin (WT sw ApoMb) and for mutated proteins with V10A, V10F, E109F, L115A, L115F, M131A, and V10AM131A; a value of 0.56 was used for the variants with W14A and W14F, 0.95 was used for sw ApoMb E109Y, and 1.21 was used for M131W (51). For amyloid fibril formation, protein solutions (5 mg/mL) were incubated at 40°C for 24 h.

Thioflavin T binding

Thioflavin T (ThT) fluorescence measurements were made using a Varian Cary Eclipse spectrofluorimeter (Agilent Technologies, Santa Clara, CA). Aliquots were taken after 24 h of incubation of protein solutions at 40°C and mixed with ThT solution before the measurements. The protein concentration was 0.5 mg/mL (28 μM); the dye concentration was 50 μM. The excitation wavelength was 450 nm. Emission spectra were recorded in the range of 460–600 nm at 25°C, and the double optical path of the cuvette was 0.3 $\times$ 0.3 cm.

Heme binding

sw ApoMb mutants were assayed for their capability of heme binding by adding hemin (1:1 ratio) to 0.15 mg/mL protein solution. Absorption spectra were recorded over the range of 350–450 nm using a Cary 100 spectrophotometer (Varian, New South Wales, Australia) with a cuvette of 1 cm optical pathlength.

Fourier transform infrared spectroscopy

Infrared spectra were recorded at 25°C on a Fourier IR-spectrometer Nicolet 6700 (Thermo Scientific, Waltham, MA) using 5 mg/mL protein

concentration. Protein samples were sandwiched between two plates made of CaF_2 with an optical pathlength of 5.8 μm. The spectra (each averaged from 256 scanning runs) were measured at a resolution of 4 cm^{-1}. Subtraction of buffer spectra and suppression of water steam spectra were conducted using the OMNIC software.

X-ray diffraction

Before measurements, sw ApoMb fibrils were placed in order, as described previously (52). Briefly, droplets of amyloid-containing solutions (5 mg/mL) were suspended between two glass sticks and allowed to air-dry for 2 days. Amyloid diffraction patterns were collected at the Institute of Protein Research using an x-ray generator Microstar with the optical system HELIOX and a detector Platinum135 CCD (X8 Proteum; Bruker-AXS, Billerica, MA), and CuKα radiation ($\lambda = 1.54$ Å). Protein samples were oriented perpendicularly to the x-ray beam using a four-axes κ goniometer.

Electron microscopy

Protein samples were negatively stained with 1% aqueous uranyl acetate solution (53). Carbon films (2–3 nm thick) on the surface of freshly cleaved mica were prepared using an electron beam evaporator (54). Electron micrographs were taken using a JEM-100C electron microscope (JEOL, Tokyo, Japan) operating at an accelerating voltage of 80 kV and providing 40,000-fold magnification. The protein concentration was 0.05 mg/mL.

Differential scanning microcalorimetry

Heat denaturation of sw ApoMb was studied using a SCAL-1 differential scanning calorimeter (SCAL) (55) with 0.34 mL cylindrical glass cells. The heating rate was 1 K/min, the temperature accuracy was $\pm 0.3^{\circ}$C, and the protein concentration was 1 mg/mL. Before the experiments, all samples were equilibrated overnight by dialysis against 10 mM of sodium phosphate buffer.

Circular dichroism

Circular dichroism (CD) experiments were performed on a Chirascan spectropolarimeter (Photophysics, Leatherhead, England) with 0.01 cm pathlength cells. The protein concentration was 1 mg/mL. Sample preparation and molar ellipticity calculations are described in Supporting Materials and Methods. Protein melting records were taken by monitoring molar ellipticity at a wavelength of 222 nm in the 5–95°C range, the temperature was controlled using a Peltier element. The heating rate was 1°C/min.

Native electrophoresis

A comparative analysis of sw ApoMb mutant propensities for aggregation was performed using electrophoresis in 9% PAGE under nondenaturing conditions. Gels were prepared according to (56) with the following modifications. The electrophoresis was performed at pH 5.5 without SDS addition. MES buffer (pH 5.5) was used both as an electrode buffer and for gel preparation. Positively charged methylene green dye, most appropriate for electrophoresis in acidic conditions, was added to the sample buffer. The monomer band staining intensity was calculated using Total Lab software.

RESULTS

Selection of replaceable amino acid residues

sw ApoMb mutants were constructed and their aggregation under nondenaturing conditions was studied to reveal factors that influence sw ApoMb amyloid formation. Our goal was to create mutants that will provide information on the effect of both protein structure stability and residue properties (hydrophobicity and charge) on amyloidogenesis. This imposes the following constraints on the point mutations.

1) They should be localized in amyloidogenic regions of the protein. We used predictions from the literature, according to which, A-, E-, and G-helices of myoglobin are such regions (30,32).
2) Substitutions should alter the stability of the protein structure. Therefore, we took into consideration the results of our previous studies on sw ApoMb folding (45) and residues predicted to be important for the folding process and conserved for all apomyoglobins (57). This yielded V10, W14 (A-helix), and L115 (G-helix) as the residues to be replaced and M131 (belonging to the nonamyloidogenic H-helix, but also conserved and important for sw ApoMb folding) as a control.
3) The mutations should cause changes in hydrophobicity and residue charge. To make an unambiguous conclusion as to the effect of hydrophobicity on protein aggregation, two residues with different hydrophobicity were substituted for the same residue: V10A and V10F, W14A and W14F, L115A and L115F, and M131A and M131W. To study the effect of the residue charge on amyloid-forming propensities, we constructed two mutants with the substitutions E109Y and E109F which, according to prediction, are supposed to provide a pronounced increase in amyloid formation (32).
4) Selection of double mutant, V10AM131A. The structure stability of all mutants described above was determined (Figs. 2, 5 *c*, and 6 *c*; Table 1). The obtained results show that mutant proteins are characterized by different degrees of destabilization; however, we did not obtain a mutant with the stability in a wide range between those of M131A and W14A variants. For selection of this mutant, we used additivity of double substitutions, which means that the effect of double substitutions on the structure stability is approximately equal to the sum of the effects of the constituent single mutations (58). Substitution V10A, which results in the least destabilization of sw ApoMb, was added to substitution M131A. The resulting mutant, V10AM131A, is characterized by the required degree of destabilization that extends the range of mutant forms and makes them appropriate for investigation of protein structure stability on aggregation.

For some of the obtained variants, it was shown previously (59) that the shape and intensity of far ultraviolet (UV) CD spectra under native conditions are close to those for the wild-type protein. These data suggest that mutations did not significantly change the native structure of the

TABLE 1 Properties of WT sw ApoMb, Its Mutants, and Their Aggregates

Protein	T_m (°C)	$f_{N\ (pH\ 5.5\ and\ 40°C)}$ (%)	$f_{I\ (pH\ 5.5\ and\ 40°C)}$ (%)	Monomer Band Staining Intensity (r.u.)[a]	A_{1620}:A_{1650} Ratio	Change in Hydrophobicity (kcal/mol)[b]	Change in β-Sheet Propensity[c]
WT	60.9 ± 0.2	83.4 ± 0.6	16.6 ± 0.6	1.00 ± 0	0.72 ± 0,01	0	0
V10A	56.7 ± 1.3	81.8 ± 0.9	18.2 ± 0.9	0.49 ± 0.01	0.82 ± 0.01	−1.2	−0.34
V10F	51.0 ± 1.5	74.7 ± 0.6	25.3 ± 0.6	0.11 ± 0.02	0.86 ± 0.02	0.8	0
W14A	47.1 ± 0.4	30.6 ± 6.1	69.4 ± 6.1	0.08 ± 0.01	0.82 ±0.01	−2.6	−0.23
W14F	55.3 ± 0.2	75.2 ± 2.2	24.7 ± 2.2	0.34 ± 0.02	0.85 ± 0.05	−0.6	0.11
E109Y	49.6 ± 0.1	71.8 ± 3.2	28.2 ± 3.2	0.03 ± 0.01	0.87 ±0.02	2.2	0.24
E109F	51.5 ± 1.4	68.1 ± 2.0	31.9 ± 2.0	0.04 ± 0.01	0.91 ±0.06	3.3	0.22
L115A	49.5 ± 0.6	63.8 ± 0.8	36.2 ± 0.8	0.07 ± 0.01	0.89 ±0.02	−1.9	−0.15
L115F	56.6 ± 0.4	74.9 ± 2.1	25.1 ± 2.1	0.26 ± 0.02	0.88 ± 0.01	0.1	0.19
M131A	47.7 ± 0.9	56.5 ± 2.4	43.5 ± 2.4	0.13 ± 0.01	0.85 ±0.02	−1.2	−0.21
M131W	58.9 ± 0.4	87.9 ± 1.7	12.1 ± 1.7	0.81 ± 0.01	0.72 ± 0.01	1.4	0.02
V10AM131A	42.9 ± 2.1	47.2 ± 4.7	52.8 ± 4.7	0.09 ± 0.02	0.83 ± 0.02	−2.4	−0.55

[a]Normalized to WT sw ApoMb.
[b]The data are from (65).
[c]The data are from (66).

protein. Similar results have been obtained for all described mutant forms.

Structural stability of WT sw ApoMb and its mutants

Our study was focused on sw ApoMb amyloid aggregation in the absence of protein unfolding. Hence, the conditions used were pH 5.5 and 40°C, because the former is maximally close to the native conditions in which sw ApoMb amyloid formation is possible, whereas 40°C provides acceleration of the aggregation, thus making it observable at physiological temperatures (37). First, it was necessary to ascertain that under these conditions, the ApoMb molecule remains folded. To do so, we assayed WT sw ApoMb and its mutants for heme-binding ability at pH 5.5. Fig. 1 a shows absorption spectra for WT sw ApoMb and its mutants after hemin addition to the solution.

The appearance of the absorption peak within the Soret band (410 nm) shows that, under these conditions, the structure of heme-binding sites in mutants is close to that in WT sw ApoMb, and that these mutants retain their functional activity (Fig. 1 *a*).

For estimation of the secondary structure content of monomeric sw ApoMb at pH 5.5 and 40°C, far UV CD spectra were measured (Fig. 1 *b*). The spectra were recorded just after the temperature increase in the cuvette without prolonged incubation of solution. For comparison, Fig. 1 *b* shows the spectra of the native and intermediate states of WT sw ApoMb, measured under conditions where these states are maximally populated: pH 6.2 and 20°C for the N state and pH 4.0 and 20°C for the I state. The intensity and shape of the CD spectrum of WT sw ApoMb at pH 5.5 and 40°C is characterized by values between those of the native (N) and intermediate (I) states, which indicates that, under these conditions, ApoMb molecules contain a pronounced secondary structure. The obtained data suggest that ApoMb molecules at the N and I states are populated, under these conditions.

Comparison of the structure stability of sw ApoMb and its mutant forms was performed using the equilibrium unfolding data. Heat melting curves and pH-induced

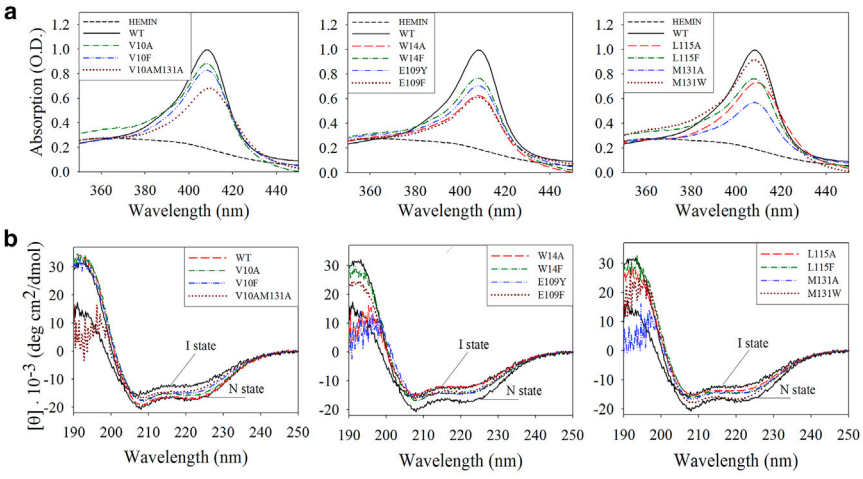

FIGURE 1 Properties of monomeric WT sw ApoMb and its mutant forms. (*a*) Absorption spectra in the Soret band region for WT sw ApoMb and its variants after hemin binding; the spectrum of hemin absorption in the absence of the protein is shown as a control. (*b*) Far UV CD spectra of WT sw ApoMb and its mutants at pH 5.5 and 40°C; spectra of the native (N) and intermediate (I) states are shown for comparison as a solid line. To see this figure in color, go online.

denaturing transitions were obtained by far UV CD, and the curves were plotted on the basis of changing molecular ellipticity at a wavelength of 222 nm, which is informative for the α-helical structure content (Fig. 2). The estimation of the protein's structure stability was carried out in two ways: 1) in accordance with the melting temperatures, and 2) on the basis of populations of the N and I states under studied aggregation conditions (pH 5.5 and 40°C). The values of melting temperatures (T_m) were obtained by fitting the melting curves to a two-state model (Fig. 2 *a*; Table 1). For description of the melting curves, the two-state model was used because the heat-denatured state of sw ApoMb is an I state. This is confirmed, first, by spectral properties of this state which are identical to those of the sw ApoMb I state; and second, since the calorimetric technique is restricted to the N→I transition for this protein, the coincidence of the middle transitions at heat denaturation curves monitored by calorimetric and CD methods indicates that actually, protein melting is a transition from its N to I state (39–41) (Fig. S1). For comparison of protein structure stability in the second way, the values of the fraction of the I state (f_I) and the fraction of the N state (f_N) at pH 5.5 and 40°C were calculated from the description of melting curves according to the two-state model (60). Under used conditions (pH 5.5 and 40°C), the native structure of ApoMb is slightly destabilized by both an increase in temperature as well by a decrease in pH. Thus, at the unfolding transitions measured at pH 5.5, the baseline corresponding to ~100% population of the N state is absent for mutants of ApoMb. Therefore, the melting curves were described as a two-state model with respect to protein destabilization at pH 5.5: f_I and f_N at baseline at a low temperature corresponded to values at pH 5.5, calculated from pH-induced transitions at 11°C (Fig. 2 *b*; Table 1). A more detailed description of these calculations is presented in Supporting Materials and Methods. The estimation of protein structure stability by both methods gives similar results, which is confirmed by the reliable correlation of T_m, with f_I and f_N values (Fig. S2).

Structural characteristics of sw ApoMb aggregates formed at 40°C and pH 5.5

Structural characteristics of sw ApoMb aggregates formed after 24 h of incubation at 40°C and pH 5.5 were obtained. The period of 24 h is enough for all the parameters to reach a plateau, thereby indicating that the aggregation process is virtually over (37). The morphology of the aggregates formed by WT sw ApoMb and its mutant forms was studied using electron microscopy (Fig. 3 *a*) to demonstrate that, under these conditions, sw ApoMb forms curved fibrils up to 100 nm in length, although a certain amount of micellar aggregate structures are present in the solution as well. The postincubation increase in ThT fluorescence indicates that the formed aggregates contain the cross-β structure (Fig. S3). Fourier transform infrared (FTIR) spectroscopy was used to investigate the secondary structure of these aggregates (61–63). Before incubation, one pronounced maximum in the FTIR spectra corresponding to α-helical and coil absorptions was recorded at 1650 cm^{-1}. After incubation, the appearance of a new peak at 1620 cm^{-1} and a shoulder at 1690 cm^{-1} shows that the cross-β structure was formed in the course of protein aggregation (Fig. 3 *b*). An x-ray diffraction technique was additionally used for identification of amyloid cross-β structure in fibrils. Investigation of fibrils formed by all mutant proteins is laborious; therefore, the diffraction pattern was obtained for one mutant form V10F, chosen as an example (Fig. 3 *c*). The presence of 4.71 and 10.10 Å reflections in the pattern allows for the unambiguous conclusion that the aggregates contain a cross-β structure, typical of amyloids.

These results are evidence that, at 40°C and pH 5.5, all the studied proteins formed aggregates, although

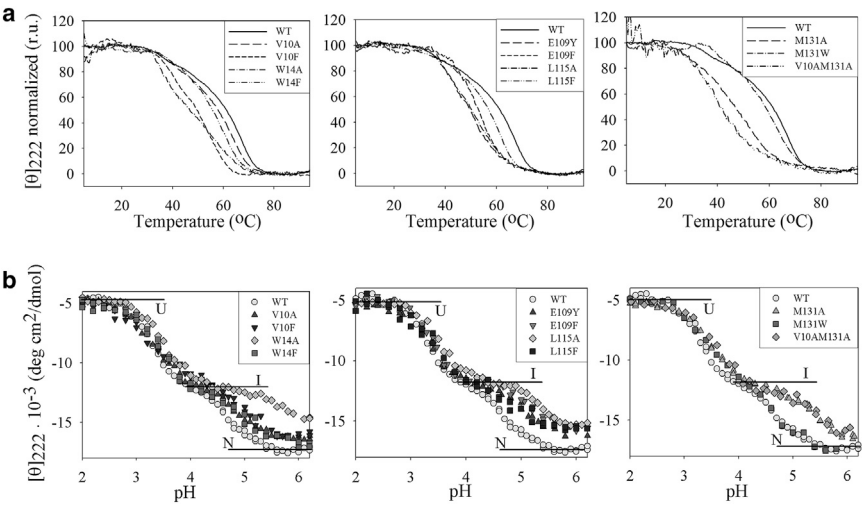

FIGURE 2 Heat melting curves at pH 5.5 of WT sw ApoMb and its mutant forms (*a*), and equilibrium pH-induced denaturing transitions at 11°C (*b*), monitored by far UV CD.

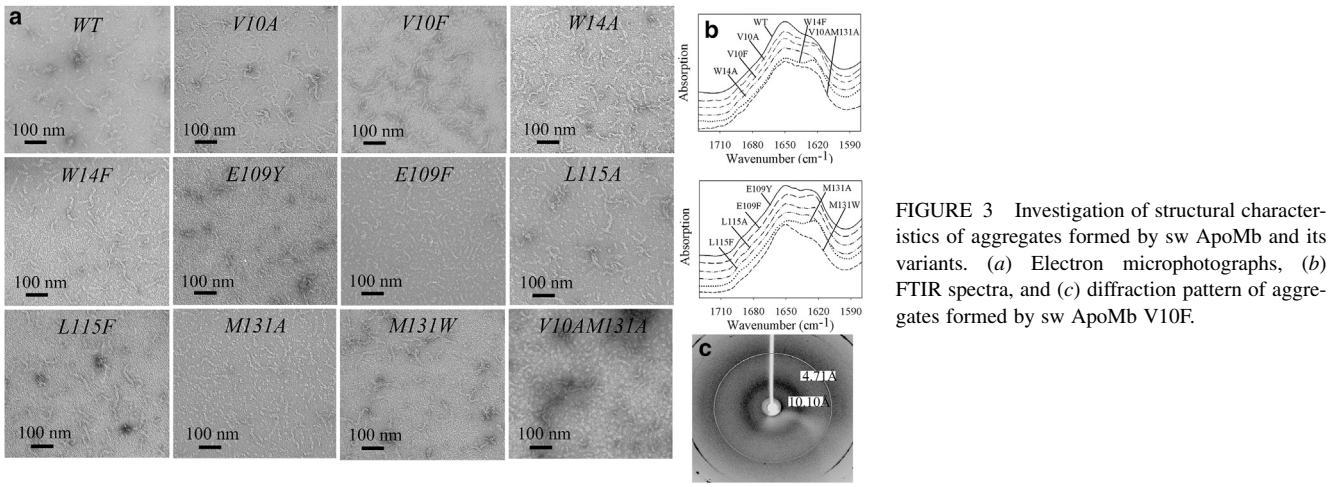

FIGURE 3 Investigation of structural characteristics of aggregates formed by sw ApoMb and its variants. (*a*) Electron microphotographs, (*b*) FTIR spectra, and (*c*) diffraction pattern of aggregates formed by sw ApoMb V10F.

the yield was different depending on the introduced mutation.

Aggregation propensities of WT sw Apo and its mutants

Previous protein aggregation studies have been focused on amyloid aggregation. Hence, only the aggregation pathway is considered rather than the aggregation landscape. Therefore, the question of what factors determine the type and structural characteristics of the formed aggregates remains unanswered. In our study, we carried out separate experiments to demonstrate the propensity of sw ApoMb mutants to form any aggregate, irrespective of its structure, and the propensity to form amyloid fibrils.

Previously, we showed that aggregation of WT sw ApoMb and its mutants is over in less than 24 h, and all recorded parameters (ThT fluorescence intensity, shape of FTIR spectra, and aggregate morphology) reach a plateau (37,64). However, during this time, some studied proteins do not completely convert to aggregates. For comparison of aggregation propensity (i.e., the content of formed aggregates after completion of the amyloid formation process), we used native electrophoresis (Fig. 4). This method has allowed for separating the monomeric protein from its aggregates. Since the latter are large, heterogeneous, and do not fully penetrate in the separating gel, it is difficult to reliably quantify them. However, the staining intensity of the monomer band can be determined with high accuracy, and serve as a basis for estimating the protein aggregation propensity. We have reported that the staining intensity of the monomeric sw ApoMb band shows linear dependence on the sw ApoMb concentration; this greatly helps in quantifying its aggregation propensity (Fig. S4).

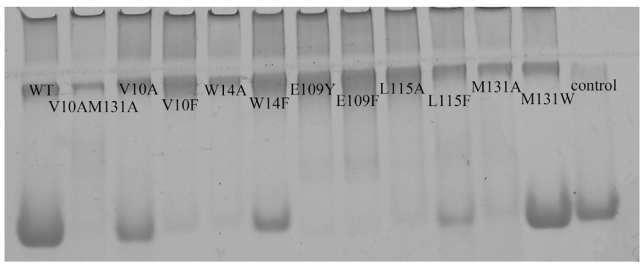

FIGURE 4 Electropherogram of WT sw ApoMb and its mutants after 24 h of incubation at 40°C. Monomeric ApoMb was applied to the last slot as a control.

To study the effect of residue substitutions on sw ApoMb aggregation propensity, after the aggregation process has completed (24 h), solutions of all the studied sw ApoMb mutants were subjected to electrophoresis in the absence of denaturant. To perform a quantitative analysis of their aggregation propensities, all samples applied onto the slots were equal in volume and concentration. Table 1 shows monomer band staining intensities for WT sw ApoMb and its mutants after 24 h of incubation.

As is already known, the main factors affecting protein amyloidogenesis under denaturing conditions are hydrophobicity, β-sheet propensity, and the charge of amino acid residues (25–29). To reveal whether sw ApoMb amyloidogenicity is dependent on these factors under the used conditions, we plotted the monomer band staining intensities as functions of changes in hydrophobicity and β-sheet propensity upon point mutations (Fig. 5, *a* and *b*) (65,66). Since the graphs show no correlation between these parameters ($r = 0.08 \pm 0.05$, $p > 0.05$ for Fig. 5 *a*; $r = 0.10 \pm 0.18$, $p > 0.05$ for Fig. 5 *b*), it may be concluded that sw ApoMb amyloidogenesis is not influenced by the above-mentioned properties under the nondenaturing conditions used. The data obtained for the mutants with charged residue mutations (E109Y and E109F) are not significantly different from data for other studied proteins.

Fig. 5 *c* shows the dependence of the protein aggregation propensity on fractions of the N and I states under aggregation-favorable conditions. It is seen that this propensity depends on the stability of the N state relative to the I state,

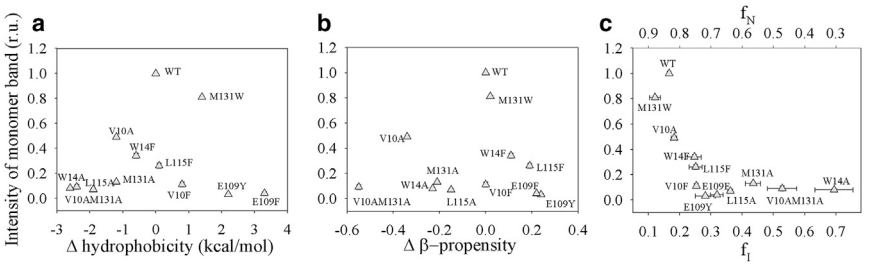

FIGURE 5 Dependence of the monomer band staining intensities on (*a*) changes in hydrophobicity, (*b*) changes in β-sheet propensity upon mutation, and (*c*) fractions of the I f_I and N states f_N at 40°C and pH 5.5. The monomer band staining intensities are normalized to that of WT sw ApoMb.

that is, the protein aggregation results from accumulation of the I state in the solution. The plateau on the graph indicates that, under the used conditions, the mutants with an I state population above 25% aggregate almost completely after 24 h of incubation at 40°C.

It was previously shown that a destabilized structure of the protein and its nonnative conformations in solution cause its aggregation (1,14,17–19). Hydrophobic groups making intramolecular contacts in the N state may be exposed to the solvent in nonnative conformational states, and form intermolecular contacts. Depending on the amino acid sequence and solvent conditions, the state of aggregate precursors can be N-like, I, or unfolded (13,14,18). The mentioned correlation between sw ApoMb amyloid-forming propensity and the I state population shows that it is mostly the I state that undergoes aggregation at 40°C and pH 5.5. Neither residue properties nor localization of the mutated residue of sw ApoMb affect the protein propensity to aggregation, which is determined by the extent of protein structure destabilization up to formation of the I state.

Amyloid-forming propensities of WT sw ApoMb and its mutants

A specific feature of amyloids is their intrinsic cross-β structure. That is why the presence of this structure has been taken as an indicator of amyloidogenicity of sw ApoMb and its mutants. For a comparative analysis of secondary structures of the mutant-produced aggregates, we recorded infrared (IR) spectra of protein solutions after their incubation at 40°C (Fig. 3 *b*).

Solutions of large aggregates are mostly heterogeneous, therefore aliquots equal in volume can contain different amounts of the protein, thereby causing differences in absorption intensities shown by IR spectra. This was the reason for β-structure quantifying as the ratio of absorption at 1620 cm^{-1} (typical of the cross-β structure) to that at 1650 cm^{-1} (typical of α-helices and coil). This allowed us to avoid sample concentration errors and to compare only the changes in the spectrum shape. The value of the selected parameter is informative to the β-structure content in aggregates (Table 1).

Fig. 6 represents this ratio, depending on changes of residue hydrophobicity and its β-sheet propensity upon mutation, and also as a function of the N and I populations of sw ApoMb mutants under aggregation-favorable conditions.

It follows from Fig. 6, *a* and *b* that sw ApoMb amyloidogenesis is independent of residue hydrophobicity and its β-sheet propensity ($r = 0.06 \pm 0.05$, $p > 0.05$ for Fig. 6 *a*; and $r = 0.19 \pm 0.18$, $p > 0.05$ for Fig. 6 *b*); mostly, amyloidogenicity of sw ApoMb and its mutants is determined by stability of the N state in relation to that of the I state (Fig. 6 *c*). Interestingly, the curve for dependence of the β-structure content in the aggregates on sw ApoMb stability is dome-shaped in this case. Hence, there exists an optimum of sw ApoMb destabilization, which is characterized by maximal amyloid-forming propensity, whereas amyloidogenicity of mutant forms with low and high destabilization degree is substantially lower. The dependences of monomer band staining intensities and the A_{1620}:A_{1650} ratio have also been plotted on the middle points of pH-induced transitions $C_{1/2}$N-I(pH) (data not shown), and these dependences are similar to those on the fractions of conformational states f_I and f_N, represented in Figs. 5 *c* and 6 *c*.

These results may be explained by comparison of Figs. 5 *c* and 6 *c*, whereby IR and native electrophoresis data are plotted. It is seen that stable proteins (wild-type and M131W) form a minor amount of amyloids, thus demonstrating their low aggregation propensities; after

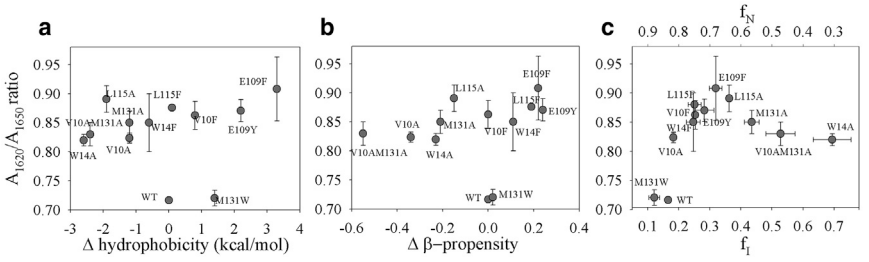

FIGURE 6 Dependence of the A_{1620}:A_{1650} ratio in IR spectra of WT sw ApoMb and its mutant forms on (*a*) changes in hydrophobicity, (*b*) changes in β-sheet propensity upon mutations, and (*c*) fractions of the I f_I and N states f_N at 40°C and pH 5.5.

incubation at 40°C for 24 h, they remain mostly monomeric. Strongly destabilized mutants aggregate completely, but form aggregates with a low cross-β structure content. This is indicative of two different sw ApoMb aggregation pathways realized under the same solvent conditions, that is, formation of amyloid fibrils and nonamyloid aggregates in the ratio determined by the stability of the N state in relation to that of the I state.

DISCUSSION

In recent years, the process of amyloid aggregation is in the focus of many studies; specifically, reports on the effect of residue mutation on amyloidogenesis are available in the literature (13,25–27,36,67–69). Some of these studies are aimed at revealing the peculiarities of aggregation of mutated proteins with substitutions underlying human diseases (67,68). The goal of other studies is examining aggregation mechanisms and approaches to their regulation. For this purpose, a large number of proteins with mutations in various regions and diverse substituting residues are used in experiments (25,26,29). However, it appears that these are mostly short peptides, intrinsically disordered proteins, and proteins studied under denaturing conditions that yielded the mechanisms of aggregation of only unfolded (feebly structured) polypeptide chains (14,18,25–27,69–71). Currently, only a few studies describe the aggregation mechanism by proteins with secondary and tertiary structures. The possibility to form amyloids from an N-like state has been shown for some proteins (12,34,35). The influence of amino acid substitutions on the rate of aggregation under N-like conditions was studied for acylphosphatase from *Sulfolobus solfataricus* and immunoglobulin light chain (13,36). For tetrameric protein transthyretin, it was shown that its amyloid-forming propensity under physiological conditions proceeds through tetramer dissociation and depends on the stability of the monomeric subunit (38). The importance of our study lies in the elucidation of the effect of mutations, both on the propensity for amyloid formation and on structural characteristics of formed aggregates by sw ApoMb under nondenaturing conditions.

The effect of residue substitution on sw ApoMb amyloidogenicity

Studies of aggregation of unfolded proteins and peptides have shown that their amyloid-forming propensities depend on the residue properties; specifically, increased hydrophobicity and the β-sheet propensities, as well as a decreased residue charge, resulted in increased amyloidogenesis. However, none of these properties has been shown to produce a notable effect on sw ApoMb aggregation under nondenaturing conditions, where fibril-forming propensities of proteins are determined by stability of the N state in relation to the I state.

As follows from the obtained results, protein stability determines not only amyloidogenesis, but also the whole protein aggregation propensity (Fig. 5 *c*). This is explained by the fact that destabilization of the sw ApoMb N state leads to an increase in the I state population. As compared to the N state, the I state contains a number of hydrophobic groups that are solvent-exposed, and therefore can form intermolecular contacts. Against the backgrounds of this difference, altered hydrophobicity of one residue plays no significant role in aggregation propensity of the entire protein. Hence, in a solution where sw ApoMb exists in different conformations with diverse aggregation propensities, its fibril-forming propensity is determined by the ratio between populations of the two states rather than by properties of an individual amino acid residue.

The I state of sw ApoMb can generate diverse aggregates

To form aggregates, for many proteins it is necessary to destabilize their N state; then, nonnative conformations prone to aggregation appear in the solution (14,17–19). In the case of sw ApoMb, its I state plays the role of an aggregate precursor (Fig. 5 *c*). However, a polypeptide chain can form diverse aggregates that differ both in morphology and secondary structure. Thus it is important to find structure-determining factors, that is, to understand whether the process of aggregation entails conformational rearrangements yielding the cross-β structure typical of amyloids or produces aggregates of a nonamyloid type. Our results show that structural characteristics of sw ApoMb aggregates formed under nondenaturing conditions depend on the population of the I state. Mutants with a medium extent of destabilization of their native structure in relation to the I form amyloids, whereas strongly destabilized proteins with an I state population above 40% form both amyloids and nonamyloid aggregates. Previously, it was demonstrated that destabilization of the N state is a prerequisite for amyloidogenesis (1,16–21). Our results show that destabilization of the N state of sw ApoMb is a prerequisite for its aggregation, but amyloid formation requires a certain extent of destabilization of its native structure.

What can explain the fact that the same protein conformation under the same conditions may act as a precursor of structurally different aggregates? The aggregate structure formed under certain conditions can be determined by both thermodynamics (stability) of aggregates and kinetics (aggregation rate) typical of a certain aggregation pathway. Since protein aggregation is a virtually irreversible process, it is most probable that the aggregation pathway is independent of stability of the formed aggregates, but is rather determined by aggregation kinetics (72). Amyloidogenesis includes several sequential steps, such as intermolecular interactions and conformational rearrangements in the formed aggregates, leading to appearance of the cross-β structure.

With the considerably increased population of the sw ApoMb I state (aggregate precursor) in solution, the aggregation rate can be so high that it exceeds the rate of conformational changes within the aggregate. This entails formation of aggregates with a low content or even absence of the β-structure. Nevertheless, competition between different aggregation pathways is currently an important and poorly understood issue in protein physics, the analysis of which is an intriguing direction of future studies in this field.

CONCLUSIONS

We have presented our experimental data concerning amyloid formation by sw ApoMb under nondenaturing conditions. It should be mentioned that currently, only a small number of publications have reported experimental results on the mechanism of aggregation of folded proteins under nondenaturing conditions; these hardly for allow an unambiguous conclusion concerning the effect of various factors on this mechanism (12,13,34–36). Different theoretical algorithms take into account properties of amino acid residues, free energy change of unfolding, and the structural context of certain regions in the protein molecule as factors affecting amyloidogenicity of folded proteins (30,73,74).

The results of our study contribute to the understanding of sw ApoMb amyloid aggregation under conditions close to physiological ones. The obtained results show that the key determinant of sw ApoMb amyloid aggregation is the protein native structure stability relative to unfolding, whereas amyloid-forming propensity under nondenaturing conditions is almost unaffected by properties of individual residues. Here, we have also shown that the protein structure stability of sw ApoMb determines not only the aggregation propensity, but also the structural characteristics of formed aggregates. Thus, we believe that our results can be helpful for understanding the mechanism of aggregation of proteins under nondenaturing conditions, and in search for regulatory mechanisms of amyloidogenesis.

SUPPORTING MATERIAL

Supporting Materials and Methods and four figures are available at http://www.biophysj.org/biophysj/supplemental/S0006-3495(17)30809-3.

AUTHOR CONTRIBUTIONS

N.S.K. and V.E.B. designed the research. N.S. K., N.B.I., V.D.V., V.V.M., A.S.G., and A.D.N. performed the research. A.D.N. and V.A.B. contributed the analytic tools and analyzed the data. N.S.K. and V.E.B. wrote the manuscript.

ACKNOWLEDGMENTS

The authors thank P.E. Wright for providing a plasmid with sw ApoMb gene, O.V. Galzitskaya and B.S. Melnik for prediction of amino acids substitutions, D.A. Dolgikh for construction of plasmids containing sw ApoMb mutants, A.K. Surin for mass-spectrometry analysis of isolated proteins, E.I. Tiktopulo for experiments on protein heat melting, S.E. Permyakov and A.S. Kazakov for assistance in measuring FTIR spectra, A.V. Finkelstein for helpful discussion of obtained results and comments on the manuscript, and E.V. Serebrova and T.B. Kuvshinkina for help in manuscript preparation.

Detailed study of amyloid formation was supported by the Russian Scientific Foundation (grant 14-24-00157). Construction of plasmids containing ApoMb mutants and protein isolation were supported by the Molecular and Cell Biology Program of the Russian Academy of Science (RAS). Initial studies of ApoMb aggregation was supported by the International Association for the Promotion of Co-operation with Scientists from the New Independent States of the Former Soviet Union (INTAS) (grant 05-1000004-7747).

REFERENCES

1. Dobson, C. M. 1999. Protein misfolding, evolution and disease. *Trends Biochem. Sci.* 24:329–332.
2. Knowles, T. P., M. Vendruscolo, and C. M. Dobson. 2014. The amyloid state and its association with protein misfolding diseases. *Nat. Rev. Mol. Cell Biol.* 15:384–396.
3. Bucciantini, M., E. Giannoni, …, M. Stefani. 2002. Inherent toxicity of aggregates implies a common mechanism for protein misfolding diseases. *Nature.* 416:507–511.
4. Taylor, J. P., J. Hardy, and K. H. Fischbeck. 2002. Toxic proteins in neurodegenerative disease. *Science.* 296:1991–1995.
5. Dobson, C. M. 2006. Protein aggregation and its consequences for human disease. *Protein Pept. Lett.* 13:219–227.
6. Chiti, F., and C. M. Dobson. 2006. Protein misfolding, functional amyloid, and human disease. *Annu. Rev. Biochem.* 75:333–366.
7. Makin, O. S., E. Atkins, …, L. C. Serpell. 2005. Molecular basis for amyloid fibril formation and stability. *Proc. Natl. Acad. Sci. USA.* 102:315–320.
8. Fändrich, M., and C. M. Dobson. 2002. The behaviour of polyamino acids reveals an inverse side chain effect in amyloid structure formation. *EMBO J.* 21:5682–5690.
9. Stefani, M. 2003. What the use of disease-unrelated model proteins can tell us about the molecular basis of amyloid aggregation and toxicity. *Ital. J. Biochem.* 52:162–176.
10. Gross, M. 2000. Proteins that convert from alpha helix to beta sheet: implications for folding and disease. *Curr. Protein Pept. Sci.* 1:339–347.
11. Chiti, F., M. Calamai, …, C. M. Dobson. 2002. Studies of the aggregation of mutant proteins *in vitro* provide insights into the genetics of amyloid diseases. *Proc. Natl. Acad. Sci. USA.* 99 (*Suppl 4*):16419–16426.
12. Soldi, G., F. Bemporad, …, F. Chiti. 2005. Amyloid formation of a protein in the absence of initial unfolding and destabilization of the native state. *Biophys. J.* 89:4234–4244.
13. Plakoutsi, G., F. Bemporad, …, F. Chiti. 2006. Exploring the mechanism of formation of native-like and precursor amyloid oligomers for the native acylphosphatase from *Sulfolobus solfataricus*. *Structure.* 14:993–1001.
14. Fändrich, M., V. Forge, …, S. Diekmann. 2003. Myoglobin forms amyloid fibrils by association of unfolded polypeptide segments. *Proc. Natl. Acad. Sci. USA.* 100:15463–15468.
15. Sirangelo, I., C. Malmo, …, G. Irace. 2002. Tryptophanyl substitutions in apomyoglobin determine protein aggregation and amyloid-like fibril formation at physiological pH. *J. Biol. Chem.* 277:45887–45891.
16. Ramirez-Alvarado, M., J. S. Merkel, and L. Regan. 2000. A systematic exploration of the influence of the protein stability on amyloid fibril formation *in vitro*. *Proc. Natl. Acad. Sci. USA.* 97:8979–8984.

17. Kelly, J. W. 1996. Alternative conformations of amyloidogenic proteins govern their behavior. *Curr. Opin. Struct. Biol.* 6:11–17.

18. Uversky, V. N., J. Li, and A. L. Fink. 2001. Evidence for a partially folded intermediate in alpha-synuclein fibril formation. *J. Biol. Chem.* 276:10737–10744.

19. McParland, V. J., N. M. Kad, …, S. E. Radford. 2000. Partially unfolded states of beta(2)-microglobulin and amyloid formation in vitro. *Biochemistry.* 39:8735–8746.

20. Canet, D., A. M. Last, …, C. M. Dobson. 2002. Local cooperativity in the unfolding of an amyloidogenic variant of human lysozyme. *Nat. Struct. Biol.* 9:308–315.

21. Hammarström, P., X. Jiang, …, J. W. Kelly. 2002. Sequence-dependent denaturation energetics: a major determinant in amyloid disease diversity. *Proc. Natl. Acad. Sci. USA.* 99 (*Suppl 4*):16427–16432.

22. Chiti, F., N. Taddei, …, C. M. Dobson. 2000. Mutational analysis of the propensity for amyloid formation by a globular protein. *EMBO J.* 19:1441–1449.

23. Raffen, R., L. J. Dieckman, …, F. J. Stevens. 1999. Physicochemical consequences of amino acid variations that contribute to fibril formation by immunoglobulin light chains. *Protein Sci.* 8:509–517.

24. Platt, G. W., K. E. Routledge, …, S. E. Radford. 2008. Fibril growth kinetics reveal a region of beta2-microglobulin important for nucleation and elongation of aggregation. *J. Mol. Biol.* 378:251–263.

25. Kim, W., and M. H. Hecht. 2008. Mutations enhance the aggregation propensity of the Alzheimer's A beta peptide. *J. Mol. Biol.* 377:565–574.

26. Chiti, F., N. Taddei, …, C. M. Dobson. 2002. Kinetic partitioning of protein folding and aggregation. *Nat. Struct. Biol.* 9:137–143.

27. Wurth, C., N. K. Guimard, and M. H. Hecht. 2002. Mutations that reduce aggregation of the Alzheimer's Abeta42 peptide: an unbiased search for the sequence determinants of Abeta amyloidogenesis. *J. Mol. Biol.* 319:1279–1290.

28. Uversky, V. N., and A. L. Fink. 2006. Protein Misfolding, Aggregation and Conformational Diseases. Part A: Protein Aggregation and Conformational Diseases. Springer Science + Business Media, New York, NY.

29. Chiti, F., M. Stefani, …, C. M. Dobson. 2003. Rationalization of the effects of mutations on peptide and protein aggregation rates. *Nature.* 424:805–808.

30. Fernandez-Escamilla, A. M., F. Rousseau, …, L. Serrano. 2004. Prediction of sequence-dependent and mutational effects on the aggregation of peptides and proteins. *Nat. Biotechnol.* 22:1302–1306.

31. Tartaglia, G. G., and M. Vendruscolo. 2008. The Zyggregator method for predicting protein aggregation propensities. *Chem. Soc. Rev.* 37:1395–1401.

32. Garbuzynskiy, S. O., M. Y. Lobanov, and O. V. Galzitskaya. 2010. FoldAmyloid: a method of prediction of amyloidogenic regions from protein sequence. *Bioinformatics.* 26:326–332.

33. Belli, M., M. Ramazzotti, and F. Chiti. 2011. Prediction of amyloid aggregation *in vivo*. *EMBO Rep.* 12:657–663.

34. Chiti, F., and C. M. Dobson. 2009. Amyloid formation by globular proteins under native conditions. *Nat. Chem. Biol.* 5:15–22.

35. Garcia-Pardo, J., R. Graña-Montes, …, S. Ventura. 2014. Amyloid formation by human carboxypeptidase D transthyretin-like domain under physiological conditions. *J. Biol. Chem.* 289:33783–33796.

36. Marin-Argany, M., J. Güell-Bosch, …, M. Ramirez-Alvarado. 2015. Mutations can cause light chains to be too stable or too unstable to form amyloid fibrils. *Protein Sci.* 24:1829–1840.

37. Katina, N. S., N. B. Ilyina, …, V. E. Bychkova. 2011. Apomyoglobin mutants with single point mutations at Val10 can form amyloid structures at permissive temperature. *Biochemistry (Mosc).* 76:555–563.

38. Quintas, A., D. C. Vaz, …, R. M. Brito. 2001. Tetramer dissociation and monomer partial unfolding precedes protofibril formation in amyloidogenic transthyretin variants. *J. Biol. Chem.* 276:27207–27213.

39. Griko, Y. V., P. L. Privalov, …, V. P. Kutyshenko. 1988. Thermodynamic study of the apomyoglobin structure. *J. Mol. Biol.* 202:127–138.

40. Griko, Y. V., and P. L. Privalov. 1994. Thermodynamic puzzle of apomyoglobin unfolding. *J. Mol. Biol.* 235:1318–1325.

41. Gast, K., H. Damaschun, …, G. Damaschun. 1994. Compactness of protein molten globules: temperature-induced structural changes of the apomyoglobin folding intermediate. *Eur. Biophys. J.* 23:297–305.

42. Hughson, F. M., P. E. Wright, and R. L. Baldwin. 1990. Structural characterization of a partly folded apomyoglobin intermediate. *Science.* 249:1544–1548.

43. Ptitsyn, O. B. 1995. Molten globule and protein folding. *Adv. Protein Chem.* 47:83–229.

44. Eliezer, D., J. Yao, …, P. E. Wright. 1998. Structural and dynamic characterization of partially folded states of apomyoglobin and implications for protein folding. *Nat. Struct. Biol.* 5:148–155.

45. Samatova, E. N., N. S. Katina, …, A. V. Finkelstein. 2009. How strong are side chain interactions in the folding intermediate? *Protein Sci.* 18:2152–2159.

46. Sirangelo, I., C. Malmo, …, G. Irace. 2004. Fibrillogenesis and cytotoxic activity of the amyloid-forming apomyoglobin mutant W7FW14F. *J. Biol. Chem.* 279:13183–13189.

47. Iannuzzi, C., S. Vilasi, …, I. Sirangelo. 2007. Heme binding inhibits the fibrillization of amyloidogenic apomyoglobin and determines lack of aggregate cytotoxicity. *Protein Sci.* 16:507–516.

48. Fink, A. L. 1998. Protein aggregation: folding aggregates, inclusion bodies and amyloid. *Fold. Des.* 3:R9–R23.

49. Jennings, P. A., M. J. Stone, and P. E. Wright. 1995. Overexpression of myoglobin and assignment of its amide, C α and C β resonances. *J. Biomol. NMR.* 6:271–276.

50. Baryshnikova, E. N., B. S. Melnik, …, V. E. Bychkova. 2005. Three-state protein folding: experimental determination of free-energy profile. *Protein Sci.* 14:2658–2667.

51. Gill, S. C., and P. H. von Hippel. 1989. Calculation of protein extinction coefficients from amino acid sequence data. *Anal. Biochem.* 182:319–326.

52. Makin, O. S., and L. C. Serpell. 2005. X-ray diffraction studies of amyloid structure. *Methods Mol. Biol.* 299:67–80.

53. Valentine, R. C., B. M. Shapiro, and E. R. Stadtman. 1968. Regulation of glutamine synthetase. XII. Electron microscopy of the enzyme from *Escherichia coli*. *Biochemistry.* 7:2143–2152.

54. Vasiliev, V. D., and V. E. Koteliansky. 1979. Freeze-drying and high-resolution shadowing in electron microscopy of *Escherichia coli* ribosomes. *Methods Enzymol.* 59:612–629.

55. Senin, A. A., S. A. Potekhin, …, V. V. Filimonov. 2000. Differential scanning microcalorimeter SCAL-1. *J. Therm. Anal. Calorim.* 62:153–160.

56. Laemmli, U. K. 1970. Cleavage of structural proteins during the assembly of the head of bacteriophage T4. *Nature.* 227:680–685.

57. Ptitsyn, O. B., and K. L. Ting. 1999. Non-functional conserved residues in globins and their possible role as a folding nucleus. *J. Mol. Biol.* 291:671–682.

58. Sandberg, W. S., and T. C. Terwilliger. 1993. Engineering multiple properties of a protein by combinatorial mutagenesis. *Proc. Natl. Acad. Sci. USA.* 90:8367–8371.

59. Baryshnikova, E. N., V. A. Balobanov, …, V. E. Bychkova. 2007. Equilibrium unfolding of mutant apomyoglobins with substitutions of conserved nonfunctional residues by alanine. *Mol. Biol. (Mosk).* 41:674–680.

60. Pace, C. N. 1986. Determination and analysis of urea and guanidine hydrochloride denaturation curves. *Methods Enzymol.* 131:266–280.

61. Chirgadze, Y. N., and E. V. Brazhnikov. 1974. Intensities and other spectral parameters of infrared amide bands of polypeptides in the alpha-helical form. *Biopolymers.* 13:1701–1712.

62. Kong, J., and S. Yu. 2007. Fourier transform infrared spectroscopic analysis of protein secondary structures. *Acta Biochim. Biophys. Sin. (Shanghai).* 39:549–559.

63. Zandomeneghi, G., M. R. Krebs, …, M. Fändrich. 2004. FTIR reveals structural differences between native beta-sheet proteins and amyloid fibrils. *Protein Sci.* 13:3314–3321.

64. Katina, N., A. Timchenko, …, V. Bychkova. 2012. Kinetics of mutant apomyoglobin association. *Macromol. Symp.* 317–318:215–226.

65. Fauchere, J. L., and V. Pliska. 1983. Hydrophobic parameters-p of amino acid side-chains from the partitioning of N-acetyl aminoacid amide. *Eur. J. Med. Chem.* 18:369–375.

66. Street, A. G., and S. L. Mayo. 1999. Intrinsic beta-sheet propensities result from van der Waals interactions between side chains and the local backbone. *Proc. Natl. Acad. Sci. USA.* 96:9074–9076.

67. Dumoulin, M., D. Canet, …, C. M. Dobson. 2005. Reduced global cooperativity is a common feature underlying the amyloidogenicity of pathogenic lysozyme mutations. *J. Mol. Biol.* 346:773–788.

68. Raimondi, S., F. Guglielmi, …, V. Bellotti. 2011. Effects of the known pathogenic mutations on the aggregation pathway of the amyloidogenic peptide of apolipoprotein A-I. *J. Mol. Biol.* 407:465–476.

69. Flagmeier, P., G. Meisl, …, C. Galvagnion. 2016. Mutations associated with familial Parkinson's disease alter the initiation and amplification steps of α-synuclein aggregation. *Proc. Natl. Acad. Sci. USA.* 113:10328–10333.

70. Cao, P., P. Marek, …, D. P. Raleigh. 2013. Islet amyloid: from fundamental biophysics to mechanisms of cytotoxicity. *FEBS Lett.* 587:1106–1118.

71. Doran, T. M., A. J. Kamens, …, B. L. Nilsson. 2012. Role of amino acid hydrophobicity, aromaticity, and molecular volume on IAPP(20-29) amyloid self-assembly. *Proteins.* 80:1053–1065.

72. Baskakov, I. V., G. Legname, …, F. E. Cohen. 2001. Folding of prion protein to its native alpha-helical conformation is under kinetic control. *J. Biol. Chem.* 276:19687–19690.

73. Tartaglia, G. G., A. P. Pawar, …, M. Vendruscolo. 2008. Prediction of aggregation-prone regions in structured proteins. *J. Mol. Biol.* 380:425–436.

74. Zambrano, R., M. Jamroz, …, S. Ventura. 2015. AGGRESCAN3D (A3D): server for prediction of aggregation properties of protein structures. *Nucleic Acids Res.* 43 (W1):W306–W313.

Biophysical Journal, Volume *113*

Supplemental Information

sw ApoMb Amyloid Aggregation under Nondenaturing Conditions: The Role of Native Structure Stability

Natalya S. Katina, Vitalii A. Balobanov, Nelly B. Ilyina, Victor D. Vasiliev, Victor V. Marchenkov, Anatoly S. Glukhov, Alexey D. Nikulin, and Valentina E. Bychkova

sw ApoMb Amyloid Aggregation under Non-denaturing Conditions: the Role of Native Structure Stability

Natalya S. Katina, Vitalii A. Balobanov, Nelly B. Ilyina, Victor D. Vasiliev, Victor V. Marchenkov, Anatoly S. Glukhov, Alexey D. Nikulin, and Valentina E. Bychkova

Institute of Protein Research, Russian Academy of Sciences, Pushchino, Moscow Region 142290, Russian Federation

SUPPORTING MATERIAL

The current paper is devoted to aggregation of sw ApoMb and its mutated forms under non-denaturing conditions. It is shown that the major factor that determines both aggregation propensity and characteristics of the formed aggregates is stability of the protein native state. Here we show additional experimental data and describe standard methods for investigation of protein folding and mathematical data processing, as well as peculiarities of these methods used in our study.

To confirm that the heat-denatured state of sw ApoMb is an intermediate state we compared the melting curves obtained by far UV CD and calorimetry (Fig. S1). Since the calorimetric technique is restricted to the N→I transition for this protein, the coincidence of the melting temperature obtained by both methods indicates that the melting of sw ApoMb is a transition from its native state to intermediate state.

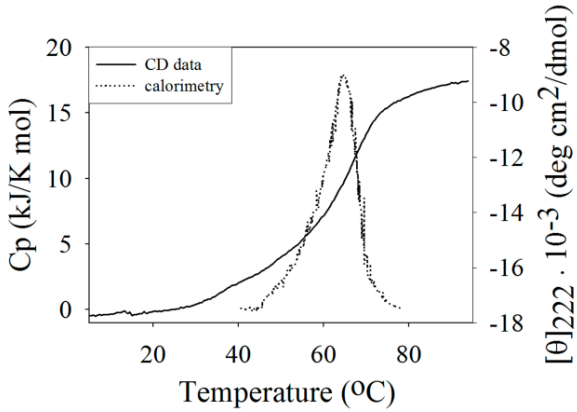

FIGURE S1 Melting curves of WT sw ApoMb monitored by far UV CD and differential scanning microcalorimetry.

To confirm that the estimation of sw ApoMb and its mutant forms structure stability in accordance with the melting temperatures and on the basis of populations of the N and I states at pH 5.5 and 40°C give a similar results we plotted the dependence of T_m on f_I and f_N. Calculated values of r and P are represented in fig. S2 and report that the T_m values correlate with f_I and f_N.

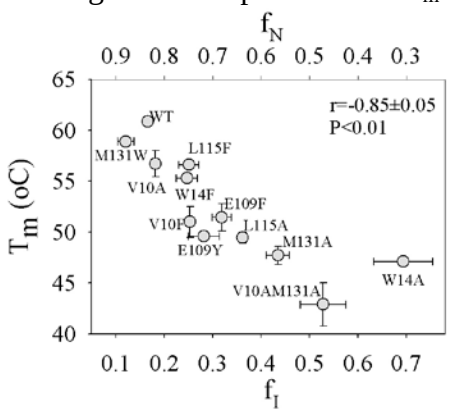

FIGURE S2 Dependence of the melting temperature (T_m) at pH 5.5 of WT sw ApoMb and its mutant forms on fractions of the intermediate f_I and the native states f_N at 40°C and pH 5.5.

For additional confirmation that aggregates formed by WT sw ApoMb and its mutant forms exhibit amyloid structure properties, the method of ThT fluorescence was used. The increase in ThT fluorescence after protein incubation at 40°C indicates that the formed aggregates contain the cross β-structure (Fig. S3).

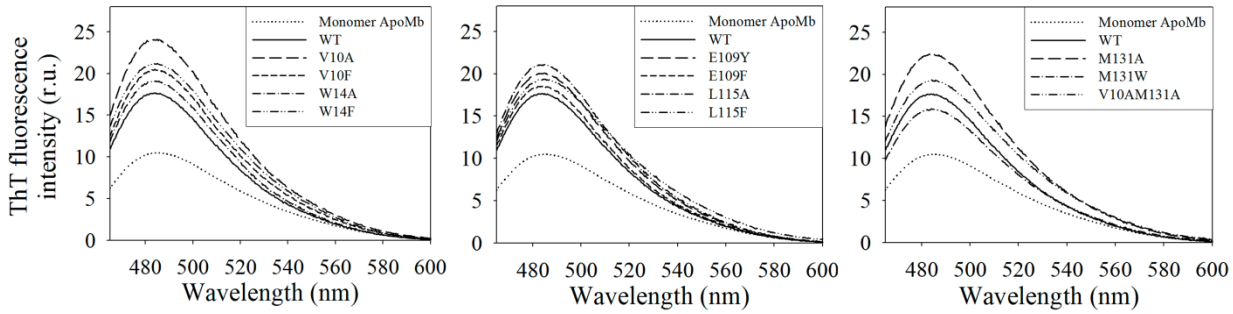

FIGURE S3 ThT fluorescence spectra of WT sw ApoMb and its mutant forms after incubation at 40°C, the spectrum of WT ApoMb before incubation presented for comparison (Monomer ApoMb).

The aggregation propensity of WT sw ApoMb and its mutant forms was determined using the staining intensity of the monomeric gel band in the electrophoregram of native electrophoresis. To be able to quantify the amount of formed aggregates according to the electrophoresis data, it was necessary to plot the concentration dependence of the gel band staining intensity and determine the shape of this dependence. Electrophoregram of monomeric sw ApoMb applied onto the slots in sequential concentrations decrease from 1.0 to 0.2 mg/ml is represented in fig. S4 *a*, all samples applied onto the slots were equal in volume. As follows from Fig. S4 *b*, the staining intensity of the monomeric sw ApoMb band shows linear dependence on the protein concentration; this helps much in quantifying its aggregation propensity.

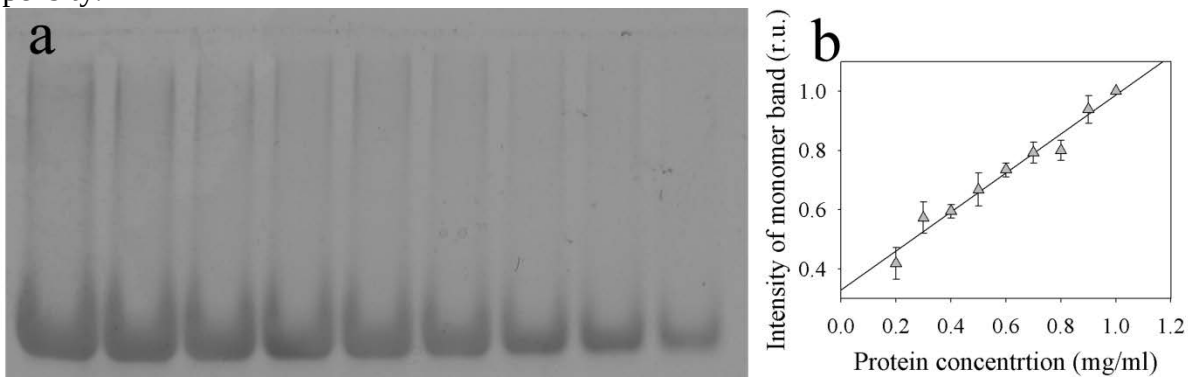

FIGURE S4 Monomer concentration dependence of the gel band staining intensity: *(a)* electrophoregram of monomeric sw ApoMb applied onto the slots in sequential concentrations decrease from 1.0 to 0.2 mg/ml; *(b)* calculated gel band staining intensity as a function of concentration of monomeric protein applied onto the slots. The monomer band staining intensities are normalized to that of sample with the concentration 1 mg/ml.

CD

Sample preparation for acidic equilibrium unfolding of WT sw ApoMb and its mutants was performed as follows: sw ApoMb was dissolved in sodium acetate buffer (NaAc), pH 6.2 (to preserve its native state), and divided into aliquots where the required pH was reached by addition of the appropriate amount of HCl.

Molar ellipticity [θ] was calculated according to the formula:

$$[\theta]_\lambda = [\theta]_\lambda \times MRW/l \times c, \qquad \text{(Eq. S1)}$$

where θ_λ is the ellipticity value measured at a wavelength of λ, mdeg; MRW is the average residue molecular weight calculated from the amino acid sequence; l is the optical path length, mm; c is the protein concentration, mg/ml. All experiments were carried out at 11°C in a buffer

system with 0.01 M NaAc. For every mutant protein, two independent experimental unfolding curves were measured.

Calculation of the native- and intermediate state fractions

Populations of the intermediate- and native states at 40°C and pH 5.5 were estimated using both the data on heat melting curves and acidic pH-induced equilibrium unfolding transitions at 11°C. The former allowed calculating conformational state populations at 11°C and pH 5.5, and then the fractions of the two states were estimated using the data on protein melting at 40°C. As it follows from acidic pH-induced equilibrium unfolding transitions, at pH 5.5, sw ApoMb molecules are in the native-like or intermediate states, but never of the sw ApoMb mutants undergo the I-U transition. Therefore, for our calculations we used the formulae for one-stage transitions (1):

$$f_{I(11℃,\mathrm{pH5.5})} = (\theta_{\mathrm{N}} - \theta_{\mathrm{pH5.5}})/(\theta_N - \theta_I), \quad \text{(Eq. S2)}$$

$$f_{N(11℃,\mathrm{pH5.5})} = 1 - f_{I(11℃,\mathrm{pH5.5})}, \quad \text{(Eq. S3)}$$

where $f_{N(11℃,\mathrm{pH5.5})}$ and $f_{I(11℃,\mathrm{pH5.5})}$ are fractions of the native- and intermediate states observed at 11°C and pH 5.5, respectively; θ_N and θ_I are the values of molar ellipticity for the native- and intermediate states, respectively, obtained from acidic pH-induced equilibrium unfolding transitions, deg cm^2/dmol; $\theta_{\mathrm{pH5.5}}$ is the value of molar ellipticity at pH 5.5, deg cm^2/dmol.

Then, basing on the results on protein heat melting at pH 5.5, we calculated fractions of the native- and intermediate states at 40°C. Since a melted conformation of sw ApoMb is its intermediate state, in these calculations sw ApoMb melting is taken to be a one-stage N-I transition. On the heat melting curve there are two base lines: one of these is observed at high temperature and consistent with the heat-denatured state, while the other is for the range from 5°C to 20°C and is consistent with the values of $f_{N(11℃,\mathrm{pH5.5})}$ and $f_{I(11℃,\mathrm{pH5.5})}$ calculated from the pH-induced unfolding transitions. Therefore, populations of the conformational states occurring at 40°C and pH 5.5 were calculated on the basis of heat melting curves using the following formulae:

$$f_{I(40℃,\mathrm{pH5.5})} = f_{I(11℃)} + [(1 - f_{I(11℃)}) \times ((\theta_{11℃} - \theta_{40℃})/(\theta_{11℃} - \theta_T))], \quad \text{(Eq. S4)}$$

$$f_{N(40℃,\mathrm{pH5.5})} = 1 - f_{I(40℃,\mathrm{pH5.5})}, \quad \text{(Eq. S5)}$$

where $f_{N(40℃,\mathrm{pH5.5})}$ and $f_{I(40℃,\mathrm{pH5.5})}$ are fractions of the native- and intermediate states at 40°C and pH 5.5, respectively; $f_{I(11℃)}$ is the intermediate state fraction at 11°C; θ_T is the molar ellipticity value of the heat-denatured state, deg cm^2/dmol; $\theta_{11℃}$ is the molar ellipticity value on the base line in the 5-20°C range, deg cm^2/dmol; $\theta_{40℃}$ is the molar ellipticity value at 40°C, deg cm^2/dmol.

Calculation of experimental errors in parameter measurements

The mean square errors of the data presented at the Table 1 were calculated as follows:

$$S = (\sum(\bar{x} - x_i)^2/(n-1))^{1/2}, \quad \text{(Eq. S6)}$$

where S is the mean square error;

$\bar{x}$ is the average value of the measured parameter: $x = \sum_{i=1}^{n} x_i /n$;

n is the number of measurements taken.

Supporting References

1. Pace, C. N. 1986. Determination and analysis of urea and guanidine hydrochloride denaturation curves. Methods Enzymol. 131:266-280.

Acknowledgements

Detailed study of amyloid formation was supported by the Russian Scientific Foundation (grant №14-24-00157). Construction of plasmids containing ApoMb mutants and protein isolation were supported by the "Molecular and Cell Biology" Program of RAS. Initial studies of ApoMb aggregation was supported by the INTAS grant № 05-1000004-7747.